

Rechargeable Li-ion batteries: Nanocomposite Materials and Applications

Yuxuan Zhang and Sunghwan Lee*

School of Engineering Technology, Purdue University, West Lafayette, IN 47907, United States

*Corresponding author: sunghlee@purdue.edu

The lithium-ion battery (LIB) is an electrochemical energy storage device that can convert between chemical energy and electric energy. Considering the perspective of energy stored per unit mass and volume, the energy density of chemical energy storage is second only to nuclear energy and higher than other forms of energy storage. At present, electrochemical energy storage has become a key supporting technology in the fields of energy, information, transportation, medical care, aerospace, intelligent manufacturing, advanced equipment, intelligent buildings, resources and environment, and national security.^{1,2} The advancements and prosperity of nanotechnology enable researchers to engineer and modify battery materials, aiming to ultimately achieve superior performance. The potential advantages of adopting nanotechnologies may include new functional reactions that are not available with bulk materials; a larger electrode/electrolyte contact area, leading to higher charge/discharge rates, and short path lengths for both electronic and Li-ion transport (enabling the utilization of materials with low electronic or low Li-ion conductivity and/or the battery operation at higher power).³ In this chapter, we will discuss some recent progress, highlighting the benefits of nanostructured cathode and anode materials, electrolyte materials, along innovative nanotechnologies utilized in LIBs.

1. Nanotechnology for Cathode Materials

In the current LIB system, the specific capacity of the whole battery is mainly limited by the capacity of the cathode material, and in the production of the battery, the cost of the cathode material accounts for more than 30% of the total cost of the entire component materials.⁴ Therefore, the preparation of low-cost cathode materials with high energy density is an important aim for the research and production of LIBs. According to the material type, cathode materials can be typically divided into three main categories sulfide-based cathode, oxide-based cathode, and phosphate-based cathode.

1.1 Sulfide-based cathode

Sulfide-based cathodes, which were the first demonstrated cathodes in the LIBs historically, have been developed for decades before the emergence of Li-containing cathodes (mainly oxide-based and phosphate-based cathodes). Recently, sulfide-based cathodes were revisited and became the promising candidate for next-generation cathode material due to their high capacity and low cost.⁵ However, these sulfide-based cathodes exhibit relatively low electronic conductivity (approximately 10^{-25} to 10^{-30} S cm⁻¹), leading to a critically limited rate capability.⁶ Additionally, the migration of polysulfide intermediates significantly compromises their cycling stability.⁷ It is widely acknowledged that enhancing the kinetic capability of sulfide-based cathode materials can be achieved by employing nanosized active materials. This nanoscale approach effectively increases the contact area of active materials with both conductive carbon and electrolyte, thereby improving electron and ion kinetics.⁸ However, the nanoscale cathode particles also present negative consequences on the battery retention capability. Lee et al. investigated the relationship between the size of the cathode particles and the battery performance by comparing the electrochemical performance of TiS₂ particles as cathode materials with three different sizes (large, middle, and small as

illustrated in the inset of Figure 14-1) in all-solid-state batteries (ASSB), where the reduced size of TiS_2 particles were achieved via high-energy ball-milling. The ASSB with the smallest-sized particles demonstrates a high-power density of over 1000 W kg^{-1} for over 50 cycles and a maximum power density of almost 1400 W kg^{-1} . The reduced-sized TiS_2 particles exposed more surface, which enabled more reaction sites and facilitated additional pathways for Li-ion transportation, leading to better utilization of active material and faster kinetics.⁹ However, these more exposed surfaces also demonstrated negative impacts on the battery performance due to the increased parasitic reactions resulting in faster degradation in capacity retention as shown in Figure 14-1.

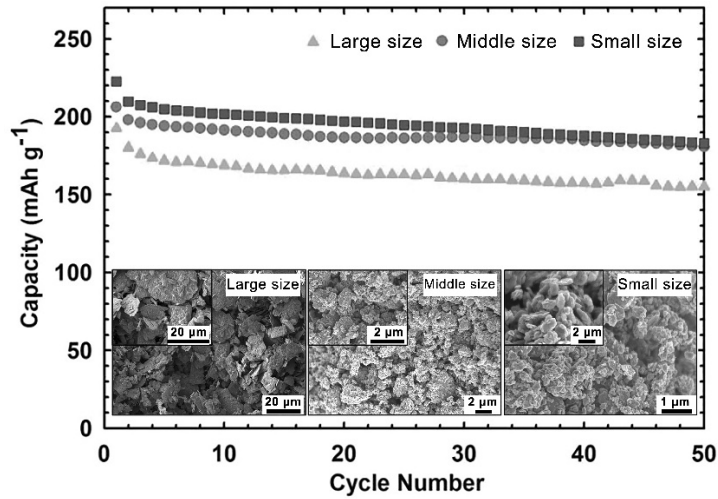


Figure 14-1. Cycling performance of ASSB with nanosized TiS_2 particles as cathode at room temperature under 2 C rate. The inset shows Scanning Electron Microscope (SEM) microstructures of TiS_2 cathode particles with three different sizes.⁹

The enhanced stability of batteries with nanoscale materials can be achieved by the engineering of crystalline orientations of the particles where only selected crystalline facets with higher stability are exposed, thereby enhancing the material's overall durability. Kovalenko et al.¹⁰ demonstrated highly crystallized FeS_2 nanoparticles with engineered facets, as indicated in Figure 14-2a. Moreover, the exposed facets of the as-synthesized nanoparticles are preferentially crystallized on orientations with (200), (210), and (311) as identified by X-ray diffraction (XRD) in Figure 14-2b. The engineering of particle shapes and crystalline orientation was achieved by careful manipulation of precursor concentration and reaction time during solution-based chemical synthesis. The controlled crystalline orientations led to higher specific capacity and rate capability while restricting capacity fading compared to bulk FeS_2 . As a result, the cathodic Li-ion storage by FeS_2 nanocrystals was demonstrated with a high specific capacity of $\geq 630 \text{ mA h g}^{-1}$ for 100 cycles (at a current of 200 mA g^{-1}), outperforming bulk FeS_2 under identical testing conditions.

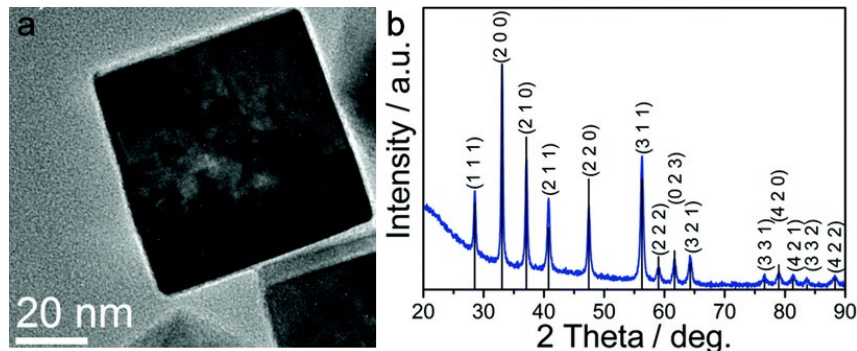


Figure 14-2. (a) Transmission electron microscopy (TEM) image of FeS_2 nanocrystals, (b) XRD pattern of FeS_2 nanocrystals.¹⁰

Nanoscale and nanostructure approaches were also applied to battery cathode materials as functional surface modifiers to promote salient improvements of the overall battery performance. Zhang et al. employed oxidative chemical vapor deposition (oCVD), which uniquely enables uniform and conformal coating of conjugated polymers as a gas-phase processing approach, to construct an ultrathin coating layer (around 40 nm) on sulfur particles to prevent the diffusion of polysulfides for Li-S batteries.¹¹ Moreover, the nanosized polymer filaments were generated between the particles aiming to enhance both the mechanical strength and electrical properties of the electrode. Consequently, the Li-S batteries leveraging ultra-thin oCVD polymer modifiers showcased a high sulfur utilization ratio of 84.4% ($\sim 1413 \text{ mAh g}^{-1}$ at 0.1 C) and capacity retention of 85% after 300 cycles ($\sim 810 \text{ mAh g}^{-1}$) at 0.5 C in its as-manufactured state (i.e., no further treatment or modification).

1.2 Oxide-based cathode

Although numerous design and modification strategies have been employed, sulfide-based materials have not yet achieved the same level of commercialization as oxide-based cathode materials, primarily due to several fundamental challenges. First, these sulfide-based cathodes are free of Li, which is synthesized in the charged state (fully delithiated) hence electrochemical lithiation was needed during the first battery discharge process.¹² Therefore, the battery voltage is the highest when cathodes are fully delithiated (Li-ion and electron removal lowers the Fermi level and increase the voltage), the accessible upper redox potential is thus limited by the oxidation state of transition metal (TM) ions during synthesis under certain atmosphere (e.g., air, oxygen, inert, and reducing atmospheres), which should not be significantly higher than the open-circuit voltage of Li-air battery ($\sim 2.91 \text{ V}$ vs Li^+/Li). Second, with a more electronegative O^{2-} (Pauling electronegativity, $\chi=3.44$ for O) compared to the S^{2-} ($\chi=2.58$ for S) in $\text{TiS}_2\text{||Li}$ metal, the average redox potential, energy density, and anodic stability of the oxide cathode have been increased.¹³ Third, the inevitable use of Li metals when Li-free cathode was adopted makes the practical application even harder due to the notorious instability and safety issues of the Li metal anode. Thus far, therefore, Li-containing cathodes based on oxides and phosphates were developed and gradually dominated the energy storage market as cathode materials.

Among oxide-based cathode materials, LiCoO_2 (LCO), LiMn_2O_4 (LMO), $\text{LiNi}_x\text{Co}_y\text{Al}_z\text{O}_2$ (NCA), and $\text{LiNi}_x\text{Co}_y\text{Mn}_z\text{O}_2$ (NCM) have been successfully commercialized for LIBs and applied on a large scale. These Li-containing cathodes enable the initial charging (i.e., delithiated) of the battery, achieving a high cell voltage of up to 5 V (vs Li^+/Li) in principle.¹⁴ In addition, these Li-containing cathode materials allow for the use of Li-free materials (e.g., graphite) as the anode in LIBs, which are safer than Li metal anode and historically critical to the success of LIBs. However, the mediocre rate performance and the instability

of the high valence state transition metal (TM) on the surface still impede practical applications requiring fast charging and high voltage conditions. In recent years, crystalline nanoparticles have been largely reported as oxide-based cathode materials, showcasing a significant improvement in rate capacities.¹⁵ LCO nanoparticles promote the de-intercalation and intercalation process of Li ions due to the very short diffusion distance from bulk to surface, compared to that of the micronized counterpart. Wu et al. synthesized LCO consisting of aggregated submicron-sized particles (about 100 nm) via the sol-gel method, demonstrating a 133 mAh g⁻¹ at the current density of 10000 mA g⁻¹ (70 C) between 0-1.05 V in aqueous electrolyte environment with high reversibility.¹⁶ In addition to augmenting the surface area, nanostructured oxide-based cathode materials particularly with selectively exposed crystalline facets were demonstrated to compensate for the reduced cycling stability that typically results from the increased number of exposed surfaces. Li et al. reported a facile synthesis of LCO nanowires via hydrothermal reaction and calcination process.¹⁷ The obtained LCO nanowires provided a specific capacity of 100 mAh g⁻¹ at a rate of 1000 mA g⁻¹ after 100 cycles, which results from their one-dimensional nanostructure and the exposure of (010) planes. As displayed in Figure 14-3a, the as-synthesized LCO nanowires are composed of many nanoparticles. The HRTEM images (Figure 14-3b, 14-3c, and 14-3d) of multiple selected regions (b), (c), and (d) of the LCO nanowire in Figure 14-3(a) show consistent lattice fringes of 0.24 nm and 0.46 nm in all the investigated locations, corresponding to the (010) and (003) facets of LCO. The appearance of (010) planes suggests the facet of LCO have been selectively exposed rather than being randomly stacked while the (003) facet has been widely reported as the typical characteristic plane of LCO cathode materials while. It is believed that the (010) plane is electrochemically active for layered LCO with the α -NaFeO₂ structure and favors fast Li-ion transportation.

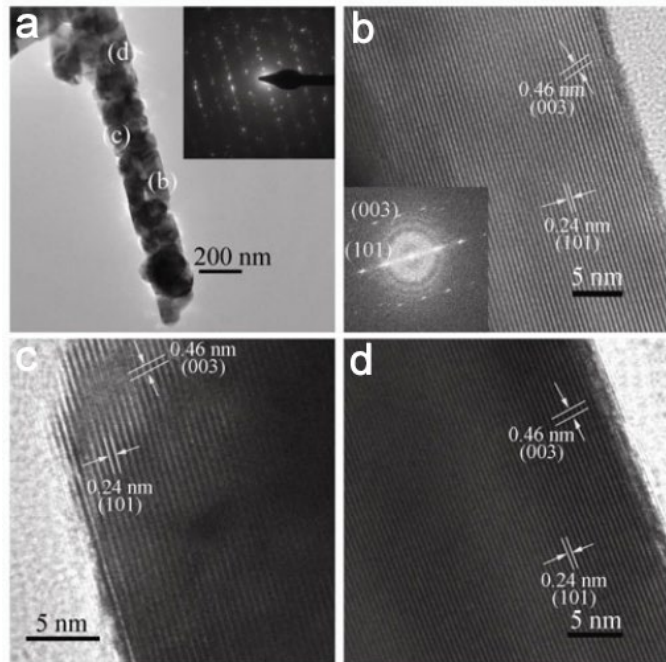


Figure 14-3. (a) TEM image of LCO nanowires; the inset image shows the electron diffraction pattern of the LCO nanowires. (b)–(d) High-Resolution TEM (HRTEM) images of several regions of the LCO nanowires (the inset image in (b) shows the Fourier Transformed diffraction pattern).¹⁷

As the particle size of oxide-based cathode materials decreases, a broader range of applications, particularly requiring more stringent kinetic conditions, becomes available. Qin et al. fabricated these spinel LMO nanoparticles through the precursor sintering process (Figure 14-4a) and employed the nanoparticle LMO

as the cathode material for aqueous lithium-ion high power-density devices.¹⁸ In the precursor sintering process in Figure 14-4a, the solution of LMO precursor was dropped on expandable graphite (EG) and dried under 180 °C at first, followed by carbonization at 700 °C, then LMO nanoparticles were obtained. SEM images show that the size of synthesized LMO nanoparticles around the dimension of 100 nm is distributed uniformly (Figures 14-4b and 14-4c). The synthesized LMO nanoparticles were fabricated into electrodes and paired with activated carbon, which delivered a high-power density of 500 W kg⁻¹ and 10,000 W kg⁻¹ with an energy density of 32.63 W h kg⁻¹ and 8.06 Wh kg⁻¹, respectively.

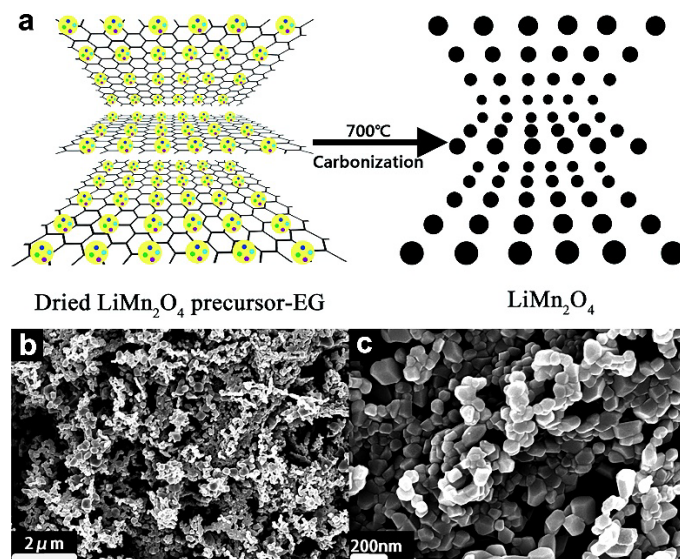


Figure 14-4. (a) Preparation process of LMO nanoparticles and (b-c) SEM microstructure images of the synthesized LMO nanoparticles.¹⁸

The surface degradation of Li-containing cathode nanoparticles becomes more significant and pronounced, compared to Li-free cathode nanoparticles. This severe degradation of Li-containing particles is attributed to the synergistic effects resulting from the large specific area and the high valence state TM at the surface. Constructing a nanoscale coating layer is considered an effective mitigation strategy to improve the electrochemical performance of the nanosized Li-containing oxide particles by restricting the parasitic reactions on their surface.¹⁹ The Al₂O₃ coating layer has been demonstrated in major cathode materials including LCO, NCA and NCM to improve cycling retention and thermal stability. Several techniques including solution process,²⁰ sol-gel,²¹ and atomic-layer deposition (ALD)²² have been showcased to build a robust Al₂O₃ coating layer on the surface of oxide-based cathode materials. Cho et al. first employed a nanometer-scale Al₂O₃ layer by the sol-gel process, successfully demonstrating its effectiveness and capability of enhancing the durability of the Li-ion battery with LCO.²³ The concentration profile in Figure 14-5a clearly shows that the Al atoms are distributed only at the particle surface region, confirming the presence of the Al₂O₃ coated on the cathode surface and no side reactions with cathode materials. Cycling data in Figure 14-5b indicate that the coated sample shows two times higher capacity retention than the uncoated sample, which is 94% of the initial capacity at the 0.5 C rate after 50 cycles (from 174 to 163 mAh g⁻¹). The observed enhancement in retention is attributed to the vital role of Al₂O₃ in enhancing the structural stability that restricts the phase transition of LCO from a hexagonal to a monoclinic phase.

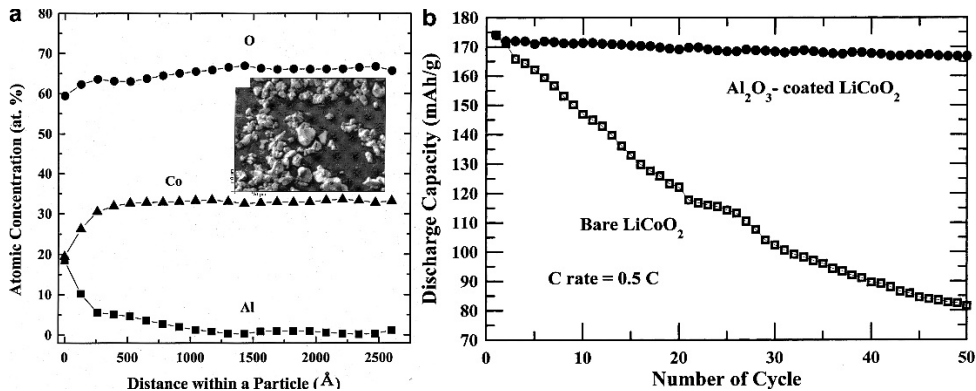


Figure 14-5. (a) Concentration profiles (Al, Co, and O) of a coated LCO particle by Auger electron spectroscopy (AES) analysis and an inset SEM image of the Al₂O₃-coated LCO particles. (b) cycle-life performances of bare and coated LCO cathodes measured at the rate of 0.5 C between 4.4 and 2.75 V in Li/LCO.²³

Phosphate nanocomposites such as AlPO₄,²⁴ Li₃PO₄,²⁵ Mn₃(PO₄)₂,²⁶ Co₃(PO₄)₂,²⁷ Fe₃(PO₄)₂,²⁸ and TiPO₄,²⁹ are also have also been practically utilized in large-scale production as cathode modification coating agents. The coated phosphate nanoparticles can generate a complex compound on the surface of the cathode materials that not only protects the surface of the cathode material but also enhances the ion conductivity of the modified cathode. As a coating layer on the cathode surface, the AlPO₄ nanoparticles would promote the formation of Co-Al-O-F species on the particle surfaces, which protects active particles from undesired side reactions with the electrolyte, possibly preventing bulk oxygen loss.³⁰

As another nanoscale coating species, polymer thin films are recently garnering much attention due to their unique functional properties including high mechanical flexibility and elasticity, adhesion capability, or the combined multifunctionalities of some of these features. Polypyrrole,³¹ polythiophene,³² polyvinylpyrrolidone,³³ and poly(3,4-ethylenedioxothiophene) (or PEDOT)³⁴ have been adopted and demonstrated effectiveness in stabilizing the electrochemical performance of oxide-based cathode materials during long cycling and high-voltage applications. The oCVD technique has been demonstrated to build ultra-thin PEDOT layers on both primary and secondary particles of the NCM cathode. The 3,4-ethylenedioxothiophene (EDOT) monomer and oxidant vapors were simultaneously introduced into a reactor and then absorbed onto the NCM particle surface as illustrated in Figure 14-6a.^{35 36} Zhang et al. employed oCVD PEDOT as unique manufacturing approach of the NCM electrode, particularly maximizing the active material loading (up to 99%) by limiting the use of binders and carbon conductors (less than 1%) in light of the adhesive capability, mechanical flexibility, and high electronic conductivity of oCVD PEDOT. TEM images in Figure 14-6b verified that both primary and secondary particles are conformally and seamlessly coated with oCVD PEDOT as marked by the yellow arrows. The energy-dispersive X-ray spectrometry (EDS) elemental mapping of a randomly selected area (red rectangle in Figure 14-6c) further confirmed the formation of PEDOT on the primary particles. The PEDOT coating layer significantly suppresses the undesired layered to spinel/rock-salt phase transformation of NCM particles during circulation and the associated oxygen loss, mitigates intergranular and intragranular mechanical cracking, and effectively stabilizes the cathode–electrolyte interface.

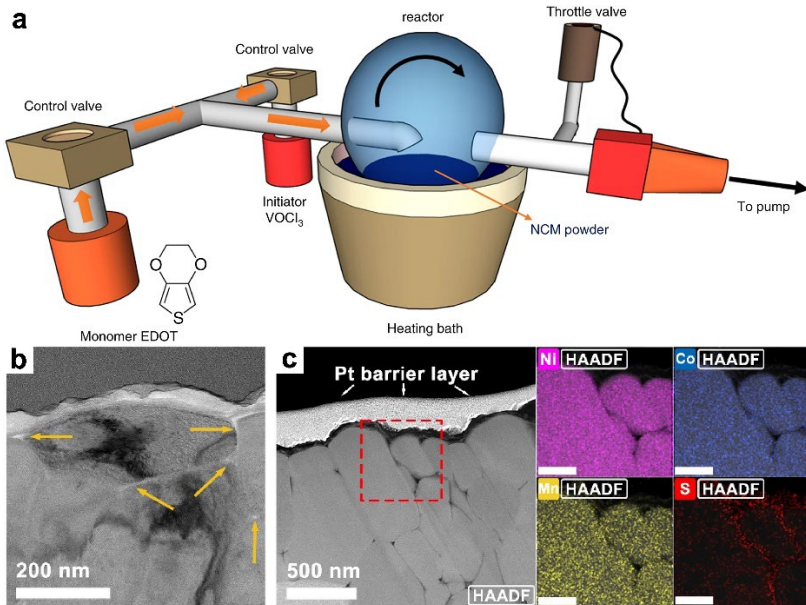


Figure 14-6. (a) A schematic diagram of the experimental oCVD setup, which relies on uniform vapor (oxidant and monomer) adsorption and subsequent *in situ* polymerization on the NCM particle (secondary and primary) surface.³⁵ (b) TEM images of cross-sectioned a PEDOT-coated NCM particle near the surface. (c) EDS mapping of the region marked in Figure 14-6c where scale bars in EDS mapping images indicate 100 nm.³⁴

1.3 Phosphate-based cathode

Lithium iron phosphate (LiFePO_4 , LFP) is another commercially available Li-containing cathode material that enables cost-effective manufacturing and long battery cycling life due to the low cost of element Fe and the stability of the olivine structure of LFP.³⁷ The sluggish electron conductivity ($\sim 10^{-9} \text{ S cm}^{-1}$) of LFP as the main drawback is largely mitigated through innovative nanotechnology approaches and hence enhances its electrochemical performance for potential use in electrical vehicles.

Armand et al. showcased an enhanced LFP with a high electrochemical performance by employing a nanoscale surface carbon coating layer, which has been widely utilized in practical applications to mitigate the issue of low electronic conductivity in LFP materials where the large surface area effectively improves the electrochemical activity of LFP.³⁸

Then with the rapid growth of nanotechnology, Takahashi et al.³⁹ and Yamada et al.⁴⁰ suggested a unique synthetic strategy of nanosized LFP crystals, which effectively shorten the diffusion pathway of Li ions and larger contact area with inactive materials especially conductive carbon in the electrode, leading to greater rate performance. Various synthetic routes and methods have been proposed in the following research such as microwave-assisted synthesis, hydrothermal synthesis, and co-precipitation for nano-sized LFP.⁴¹

Currently, oxide-based cathode materials and phosphate cathode materials dominate the market from portable electronics to electric vehicles. Nevertheless, the urgent need to increase energy density while simultaneously ensuring the safety and reliability of batteries is becoming increasingly critical. Central to this challenge is the improvement of either the specific capacity or the operational voltage of cathode materials. The primary developmental strategies for cathode materials are focused on the progression of various derivative materials from sulfide-based and oxide-based cathodes, which includes the creation of

nanocomposites, nano-coating layers, and nanocrystalline structures through the utilization of multiple advanced nanotechnologies.

2. Nanotechnology for Anode Materials

Anode materials, as crucial as cathode materials, play an indispensable role in achieving enhanced energy and power densities, cycling performance, and ensuring reliable safety of LIBs.

The selection of anode materials may consider the following criteria⁴²⁻⁴⁴: (1) The redox potential for the Li insertion/extraction reactions needs to be low, ensuring compatibility with the output voltage of LIBs. (2) Minimal variation of electrode potential during Li-ion insertion and extraction is preferred for maintaining a stable operating voltage. (3) A high reversible capacity and hence high energy density in LIBs need to be attained. (4) The structural stability of anode materials during Li-ion insertion and extraction is required for a superior cycling performance of LIBs. (5) If the Li insertion potential is below 1.2 V vs. Li⁺/Li, a dense and stable solid electrolyte interface (SEI) should form on the anode surface, preventing continuous electrolyte reduction and Li consumption at the anode. (6) The low impedance for the transportation of electrons and Li-ions is to be secured to enable a high rate of charge/discharge and efficient low-temperature performance. (7) Anode materials are expected to maintain their chemical stability after circulation, reducing the self-discharge rates of LIBs. (8) Environmental sustainability is crucial to anode materials by minimizing the pollution and toxicity within the production and disposal processes. (9) A simple and scalable manufacturing process with low production costs is a fundamental factor in the large-scale production of anode materials. The principal challenge in developing new anode materials lies in developing substances that exhibit one or more exceptional characteristics (such as ultrahigh capacity and low cost) while simultaneously securing other performance (such as fair safety and fast charging capability). Hence, the viability of material for battery applications hinges on whether its least effective performance meets the minimal application requirement, which is the so-called 'barrel effect'. Despite the exploration of thousands of anode materials over the past two decades, only a handful have achieved commercial application.

Presently, the most commonly used commercial anode materials for LIBs, offering the best overall performance that aligns with the aforementioned prerequisites, fall into two main categories: (1) artificial or naturally modified graphite with hexagonal or rhombic layered structures, and (2) Li₄Ti₅O₁₂ (LTO) with a cubic spinel structure. Other anode materials such as hard carbon-, soft carbon-, and silicon-based anode materials take only a small global market share (<1%).⁴⁵

2.1 Graphite anode

As the most commonly used anode materials, graphite anode materials have been extensively investigated and modified through various methods by constructing nanostructure materials such as nanoparticles, nanowires, and nanofibers as well as building nanoscale layers on microscale graphite particles. However, the low specific capacity of graphite anode needs to be enhanced for the implementation of next-generation batteries. Advanced nanotechnology approaches have been reported to improve the specific capacity of graphite anode. Kaiser and Smet created a superdense ordering of lithium between two graphene layers with a thickness of several nanometers with a specific capacity of more than 1000 mAh g⁻¹, indicating the potential beyond a capacity of 372 mAh g⁻¹ in graphite layers.⁴⁶ The reversible high capacity of this superdense ordering lithium graphene is attributed to the formation of LiC or Li₂C₂ compounds in graphite. In addition, controlling the nanostructures of graphite was also suggested as another promising way of improving its specific capacity. The capacity enhancement is attributed to the increased Li⁺ storage

capability of the engineered nanovoids and grain boundaries in the graphite anode, which plays a favorable role in controlling the discharge depth as schematically illustrated in Figure 14-7 since these nanostructures are able to absorb Li ions for further discharge.⁴⁷

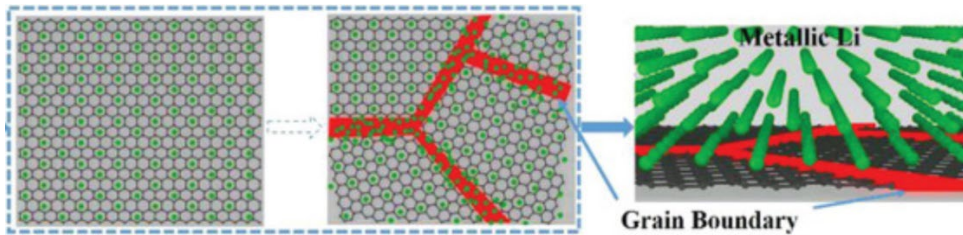


Figure 14-7. Schematic representation of lithium-storage mechanism in lithiation of graphite.⁴⁷

Despite graphite anode materials having met most of the fundamental requirements of various energy storage devices, commanding a dominant 97% share of the global anode market in LIB applications, the low chemical diffusion coefficient (approximately 10^{-10} to 10^{-11} $\text{cm}^2 \text{ s}^{-1}$) and significant volume variation (around 12%) of graphite anode materials contribute to a sluggish rate capability, which is a major drawback, particularly in fast-charging scenarios.

2.2 Li₄Ti₅O₁₂ anode

In contrast, LTO, another widely used anode material, presents much higher chemical diffusion coefficients (approximately 10^{-8} to 10^{-9} $\text{cm}^2 \text{ s}^{-1}$) and a considerably lower volume variation (about 1%), showcasing a promising alternative for fast-charging applications. Theoretically, the rate capability of the entire battery can be significantly increased by decreasing the size of the LTO materials due to the larger electrode-electrolyte contact area and shorter Li-ion diffusion pathways.⁴⁸ Tarascon and Shukla et al. synthesized nanocrystalline LTO via the single-step-solution combustion method, which involves redox reaction between the oxidizer ($\text{TiO}(\text{NO}_3)_2$ and LiNO_3 in this case) and the fuel (glycine in this case), and verified the mechanism for the first time.⁴⁹ In Figure 14-8, the synthesized nanocrystalline LTO exhibited superior high-rate performance as the anode of LIBs, which is ascribed to the nano and highly porous morphology of the LTO, leading to short diffusion paths for Li-ion and the sufficient infiltration of the non-aqueous (i.e., organic liquid) electrolyte.

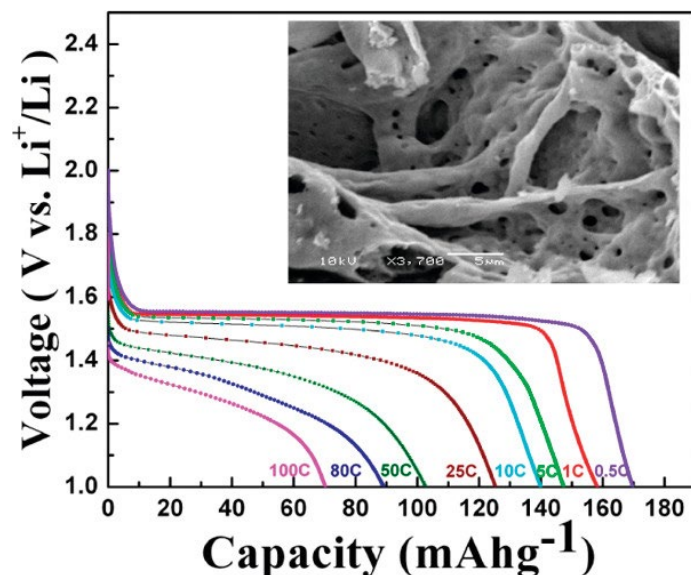


Figure 14-8. Capacity-voltage profile at different rates for nanocrystalline LTO synthesized by the combustion method. Inset shows scanning electron micrographs (SEM) for the produced nanocrystalline LTO.⁴⁹

Subsequently, synthesis methods for nanocrystalline LTO, including sol-gel, microwave-assisted, and hydrothermal techniques, have been demonstrated to effectively enhance the rate capability of LTO anode materials. Nanoscale modification approaches aiming for high-rate capability such as constructing functional thin coating layers have also been extensively investigated. Xia et al. demonstrated carbon-coated (~6 nm) LTO particles as anode that exhibited a reversible capacity of 160 mAh g⁻¹ at 0.2 C and shows remarkable rate capability by maintaining 79% of the capacity at 20 C, as well as excellent cycling stability with a capacity retention of 95% after 1000 cycles at 1 C rate.⁵⁰ This battery performance enhancement is attributed to the improved conductivity and protectivity of the thinly coated carbon layer. Although LTO operates at a higher voltage, which reduces the battery's energy density, its exceptional cycling and rate performance provide a notable safety advantage, outperforming graphite anodes. This advantage has led to an irreplaceable demand for LTO electrodes, particularly in the areas of power batteries and energy storage stations, requiring fast charging capability and long durability. LTO holds a niche yet crucial position in the global anode market, accounting for about 1% to 2%, despite its relatively low capacity of 175 mAh g⁻¹.⁵¹

2.3 Si-based anode

Apart from the graphite and LTO anodes, the remainder of the anode market is increasingly dominated by a rising star in the field: Si-based anode materials. Si-based materials have been considered as one of the most attractive anode materials for LIBs, not only because of their high gravimetric (4,200 mAh g⁻¹, calculated based on theoretical Si) and volumetric capacity (2400 mAh cm⁻³, calculated based on Si), but also due to its abundance, cheapness, and environmentally benign property.⁵² However, it suffers from fast capacity fading, which critically hampers the application of Si-based anode materials. The Si-based anode material has a large volume change (320%) during the lithium storage process, which leads to the detachment of the active material from the conductive network and the pulverization of the Si-based materials.⁵³ Further studies have confirmed that this significant volume expansion is mainly due to the relatively fast diffusion of Li-ion along the (110) orientation in crystalline Si, which leads to a preferential expansion in that direction, resulting in cracks in the electrode material, and deteriorating the cycling performance.⁵⁴ It has been found that reducing the size of Si-based materials plays an important role in developing the high-performance Si-based anode. Hence, nanomaterials have the genuine potential to make a significant impact on improving the electrochemical performance of Si-based anode, as their reduced dimensions enable far higher intercalation/deintercalation rates and minimize the effect of the direction-preferential expansion. Cui et al. synthesized Si nanowires which were grown directly on the metallic current collector substrate, accommodating for the large volume change by limited diameter and providing 1D electronic pathways, allowing for efficient charge transport (Figure 14-9a).⁵⁵ The Si nanowires display high capacities of 3,000 mAh g⁻¹ at 0.2 C rate and even a reversible capacity of over 2,100 mAh g⁻¹ at 1 C as shown in Figure 14-9b. Si nanotubes (1D structure), prepared by chemical vapor deposition, which is a widely accepted method to produce Si-based anode materials, also demonstrated elevated performance compared with the micro-sized Si anode materials.

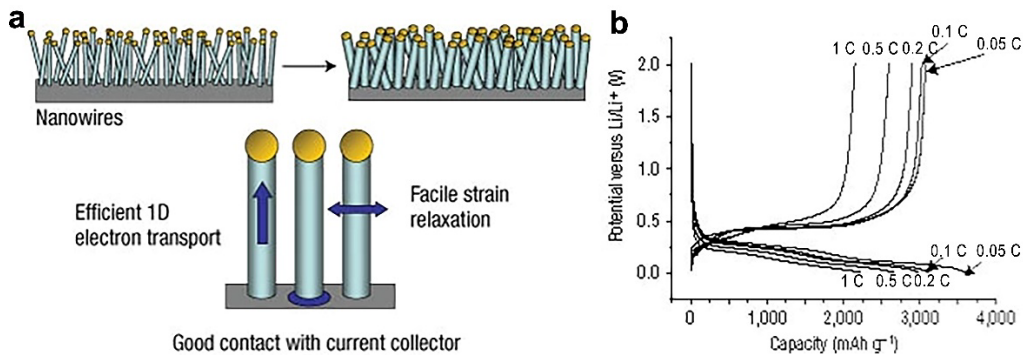


Figure 14-9. (a) The schematic of Si nanowire anode with the current collector, allowing for efficient 1D electron transport down the length of every nanowire. (b) The voltage profiles for the Si NWs cycled at different power rates. The 0.05 C profile is from the second cycle.⁵⁵

Pioneering works have shown that decreasing the dimension of Si anode materials to the nanoscale allows for the material to withstand large de-lithiation strains without fracture. However, the cycle life of nano-sized silicon is still limited due to the unstable SEI on the surface. Modifications based on nanoengineering have been proposed to construct a durable surface for Si-based anode materials. One representative work by Cui et al. showcased hollow and yolk-shell structures of Si pomegranate-like composites coated with conductive materials, establishing a potential way to solve the limited cycle life issue. They designed a novel secondary structure for Si anode materials, as shown in Figure 14-10a.⁵⁶ Such a design has multiple advantages: (1) the nano-sized primary particle and the well-defined internal void space allow the silicon to expand; (2) the carbon framework functions as an electrical highway so that all nanoparticles are electrochemically active; (3) carbon completely encapsulates the entire secondary particle, limiting the SEI film formation on the outer surface, which not only restrict the amount of SEI, but also retains the internal void space for Si expansion; and (4) the issues due to high surface area and low tap density of Si-based anode, when nano-sized primary features are introduced, are partially mitigated. The reversible capacity of Si-based composite materials reaches 2,350 mAh g^{-1} at a rate of 0.05 C, and after 1,000 cycles, over 1,160 mAh g^{-1} capacity still can be obtained (Figure 14-10b). The average Coulombic efficiency from the 500th to 1,000th cycles of the Si pomegranate is as high as 99.87 %, indicating that the SEI of the Si-based composites is highly stable.

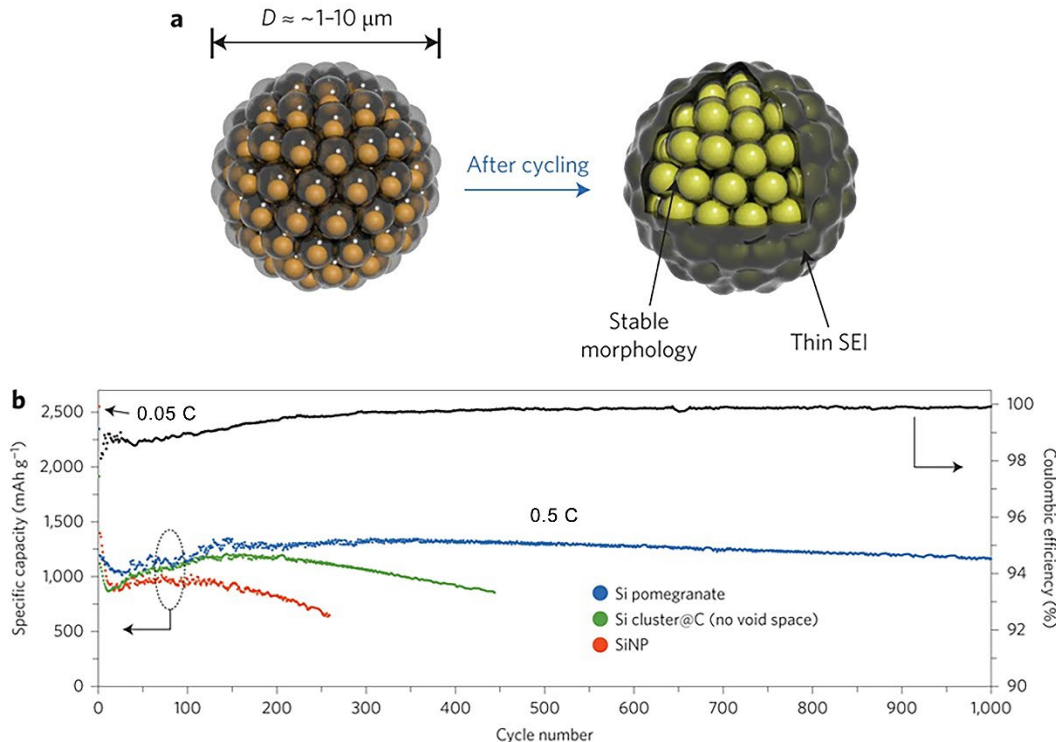


Figure 14-10. (a) Three-dimensional view of one pomegranate microparticle before and after electrochemical cycling (in the lithiated state). (b) Reversible delithiation capacity for the first 1,000 galvanostatic cycles of the silicon pomegranate and other structures tested under the same conditions. Coulombic efficiency is plotted for the silicon pomegranate only.⁵⁶

Although Si anodes have garnered considerable interest for their high capacity, researchers have extensively modified them, particularly with nanomaterials like nanoparticles and nanowires, which significantly improve cycling performance.⁵⁷ It's important to note that performance tests of these nanomaterials are primarily conducted in half-cells, which were often conducted under a large rate (0.5 C or 1 C) with low mass loading (less than 1 mg cm⁻²). When charging and discharging at lower rates (0.1 C or 0.2 C), the large specific surface area of nanomaterials can lead to the formation of a substantial amount of SEI with the consumption of the limited lithium source in the battery, leading to a significant decrease in both the energy density and cycle life of the full battery in practical applications. Therefore, research on Si anodes needs to continue focusing on two key aspects: mitigating bulk deformation and stabilizing the SEI.

Although numerous modifications have been made on Si anode materials, a significant challenge faced by these alloy anode materials is the substantial volumetric change which is directly proportional to their discharge capacity. Practical applications require that the volume of battery cells undergo minimal change (generally $\leq 5\%$, with a maximum allowance of 30%). Consequently, the advantage in volumetric energy density that alloy anodes have over graphite anodes is considerably less pronounced in practice than theoretical calculations suggest.⁵⁸ In contrast, the issue of volume expansion is not as significant for lithium metal anodes. In the most state-of-the-art research, new types of batteries, including rechargeable lithium metal batteries, all-solid-state lithium batteries, lithium-sulfur batteries, and lithium-air batteries, are under intensive research. It is foreseeable that despite nearly half a century of study, lithium metal stands a strong chance of becoming the ultimate solution for high-energy-density rechargeable lithium battery anode materials in the near future.

Currently, it is undeniable that nanostructured anode materials initiated a new paradigm in the development of rechargeable batteries in terms of their performance. In principle, the nano structural anode materials facilitate the transport for both Li ion and electron by providing shorter diffusion paths and larger specific area for the cation desorption/insertion. Additionally, the nanostructure materials are capable of providing accommodation to the expansion of anode materials during lithiation (e.g., in Si anode). However, significant limitations were also presented when nanomaterials were adopted. First, the low volumetric efficiency, owing to the large surface area and porous structure nanomaterials have low packing density compared to the micronized anode particles. Then, implementing nanomaterials anodes produces thicker SEI layers especially in Si anode, which consumes limited Li ions in the battery and increases the internal impedance, leading to a fast performance failure. Last but not least, the synthesis of nanomaterials are generally complex and limited to be applied to pilot line, making it unfavorable for mass production. It is expected that anode nanomaterials will be commercially available and fulfill the high requirements of modern applications by addressing these issues.

3. Nanotechnology for Electrolyte Materials

As a critical component of LIBs, the electrolyte, mainly consisting of non-aqueous electrolytes and solid-state electrolytes (SSEs) serves as the conductor for the Li-ion transmission between the cathode and anode, generally described as the "blood" of LIBs.⁵⁹ Non-aqueous electrolytes, comprising organic solvents, lithium salts, and additives, dominate almost the entire market share of LIBs at the current stage while SSEs are widely regarded as the future of electrolyte materials, largely due to their enhanced safety features and the potential to facilitate the application of higher energy-density lithium metal batteries.⁶⁰ Contrasting with the inherently electron-insulating nature of organic solvents in non-aqueous electrolytes, the selection of SSEs requires a focus on materials that are not only highly ion-conductive but also effectively electron-insulating. Currently, SSEs are broadly categorized into three types based on their composition: organic SSEs, inorganic SSEs, and hybrid organic-inorganic SSEs.⁶¹

3.1 Non-aqueous electrolyte

It has been evidenced that nanomaterials can improve the properties of conventional non-aqueous electrolytes in LIBs. Specifically, the incorporation of powders, particularly in nanoparticulate form, of compounds like Al_2O_3 , SiO_2 , and ZrO_2 into non-aqueous electrolytes, has been shown to increase conductivity by up to a factor of six as indicated in Figure 14-11.⁶²

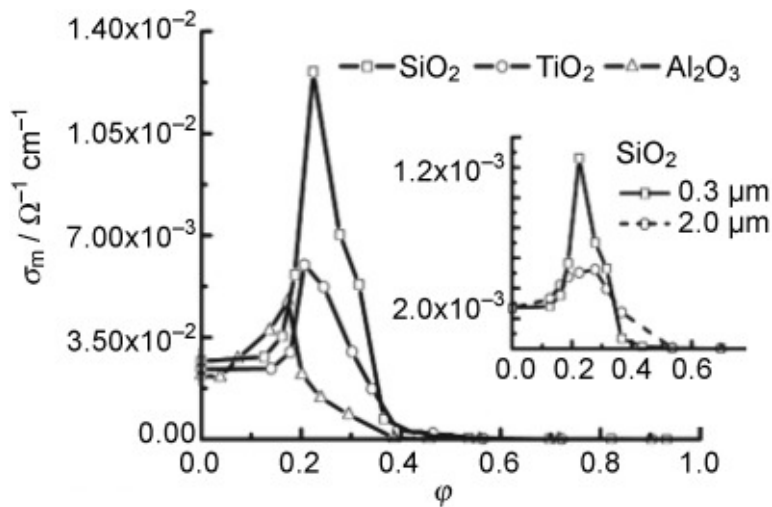


Figure 14-11. Variation of composite conductivity (σ_m) versus volume fraction (ϕ) of various oxides (particle size, $2r \approx 0.3 \mu\text{m}$) with different surface acid-base characters at room temperature.⁶²

The anisotropic forces at the interface between the non-aqueous electrolyte and solid particles differ inherently from the isotropic forces present within the bulk of either medium. Space-charge and dipole effects occur at the interface, leading to alterations in the equilibrium between free ions and ion pairs, consequently affecting the conductivity. Generally, these effects are amplified by specific adsorption (e.g., chemisorption), for instance, the adsorption of anions on the particle surface, which further promotes the dissociation of ion pairs. The larger the surface-to-volume ratio (i.e., the smaller the particles), the more pronounced the effect per unit mass of powder. As long as there is a sufficient proportion of powder to ensure percolation from one particle surface to another, this enhanced local conductivity can translate into improved long-range conduction throughout the electrolyte. Due to the significant quantity of powder required and its consequent impact on mechanical properties, these materials have been aptly termed as "soggy sands."⁶² However, the progress in lithium battery technology relies on the replacement of the conventional non-aqueous electrolyte with an advanced solid-state electrolyte.

3.2 Solid-state electrolyte

To achieve this goal, many lithium-conducting polymers have been prepared and characterized. The greatest attention has undoubtedly been focused on poly(ethylene oxide)-based (PEO-based) solid polymer electrolytes.⁶³ These electrolytes are formed by the combination of PEO and lithium salt, which are often referred to as true solid polymer electrolytes as they do not contain plasticizing solvents. PEO-based solid polymer electrolytes exhibit several distinct characteristics, including low cost, good chemical stability, and safety. However, they also present certain challenges. Their conductivity is high only at temperatures above 70 °C, which limits the practical application range of the associated polymer battery. Additionally, the conductivity is primarily due to anion movement (with the lithium transference number generally being low, in the range of 0.2-0.4), which may lead to concentration polarization, thereby limiting the rate (power) performance of the battery.⁶⁴ Accordingly, many attempts have been made to overcome these drawbacks. An interesting approach, which leads to an important enhancement of the transport properties of the PEO-based SSEs, is based on dispersion within the polymer matrix of nanoparticulate ceramic fillers, such as TiO₂, Al₂O₃, and SiO₂. There are obvious analogies with the addition of nanoparticles to non-aqueous electrolytes (amorphous solid-state polymers are viscous liquids) although there are also important differences. This new class of SSEs has been referred to as nanocomposite polymer electrolytes.⁶⁵ It has been demonstrated that one of the roles of the filler is that of acting as a solid plasticizer for PEO, by

inhibiting chain crystallization upon annealing in the amorphous state at 70 °C. This inhibition leads to the stabilization of the amorphous phase at lower temperatures and thus to an increase in the useful temperature range for the electrolyte conductivity. It is important to point out that the development of solid-state polymer electrolytes that conduct only cations is considered of prime importance in order to promote the application of lithium metal batteries.⁶⁶ Attempts, mainly directed toward immobilization of the anion in the polymer structure, have been reported in the past. However, recent research pointed out that immobilizing the anion generally depresses the overall conductivity of solid-state polymer electrolytes.

The nanocomposite approach appears to be more effective in enhancing the conductivity of the solid-state electrolyte, as in this case, the dispersion of an appropriate ceramic filler enhances the lithium transference number without inducing a drastic depression in the electrolyte conductivity. A solid-state electrolyte composite consisting of PEO/LiTFSI and Li-ion conducting Al-doped $\text{Li}_{6.75}\text{La}_3\text{Zr}_{1.75}\text{Ta}_{0.25}\text{O}_{12}$ (LLZTO) particles was demonstrated to achieve the moderate Li-ion conductivity ($1.12 \times 10^{-5} \text{ S cm}^{-1}$ at 25 °C), which was nearly 10-fold higher than that ($1 \times 10^{-6} \text{ S cm}^{-1}$) of its undoped counterpart.⁶⁷ This solid-state electrolyte obtained a high Li-ion transference number of 0.58, much higher than is seen in regular polymer electrolytes and common liquid electrolytes (typically 0.2–0.4).^{68,69} As indicated in Figure 14-12, on the one hand, the active ceramic filler serves as a rigid part to enable a uniform lithium deposition and offers ultimate protection at extreme temperatures. On the other hand, the polymer-Li salt substrate acts as a soft part to adapt the changes in the electrode for maintaining a closely contacted interface and sufficient cross-boundary ion transportation. Consequently, this SSE shows excellent flexibility and good resistance to Li dendrites.⁶⁷

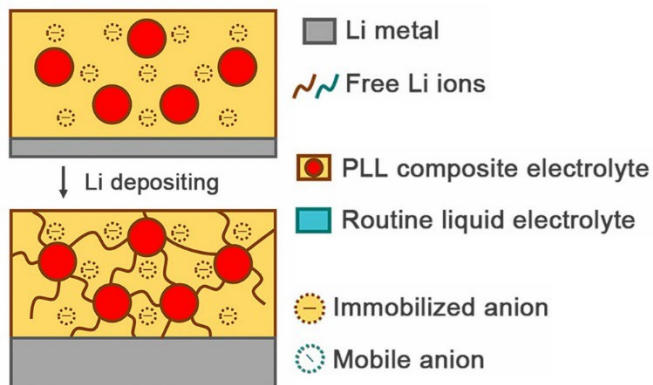


Figure 14-12. Schematic of the electrochemical deposition behavior of the Li metal anode with the solid electrolyte with immobilized anions.⁶⁷

The addition of more LLZTO in a polymer electrolyte matrix (i.e., PEO) leads to a transition from “ceramic-in-polymer” to “polymer-in-ceramic”. The highest ionic conductivity ($1.17 \times 10^{-4} \text{ S cm}^{-1}$ at 30 °C) is achieved with 10 wt.% of LLZTO particles. When the LLZTO loading reaches 85 wt.%, its mixture with PEO and PEG demonstrates excellent flexibility as a film, which can survive bending and twisting tests.⁷⁰ In addition to optimizing the composition of the solid-state electrolyte, stabilizing the interface between the electrode and electrolyte with reduced contact resistance is vital to achieve elevated battery performance. Constructing a nanoscale layer at the electrolyte/electrode interface was proposed as an interface modification strategy to limit the redox reaction between the electrolyte and the electrode as well as to reduce the high interfacial resistance. An ultrathin Al_2O_3 layer, prepared via atomic layer deposition, on garnet-like $\text{Li}_7\text{La}_{2.75}\text{Ca}_{0.25}\text{Zr}_{1.75}\text{Nb}_{0.25}\text{O}_{12}$ (LLCZN) was demonstrated to effectively improve the wetting and stability of garnet SSEs and leads to a significant decrease in interfacial impedance from $1,710 \Omega \text{ cm}^2$ to

$1 \Omega \text{ cm}^2$ (Figure 14-13a and 14-13b).⁷¹ The enhanced performance of an artificial interface can potentially be attributed to several factors. Firstly, creating an artificial interface on SSEs forms a conformal boundary between the SSEs and lithium metal, thereby enhancing the physical contact between the SSEs and the electrode. Secondly, the stabilized interface shields the parasite reactions between SSEs and the electrode, resulting in a longevity application. Lastly, an ultrathin artificial interface layer does not compromise efficient pathways for Li-ion transport through the interface, sustaining the overall utilization ratio of the material.

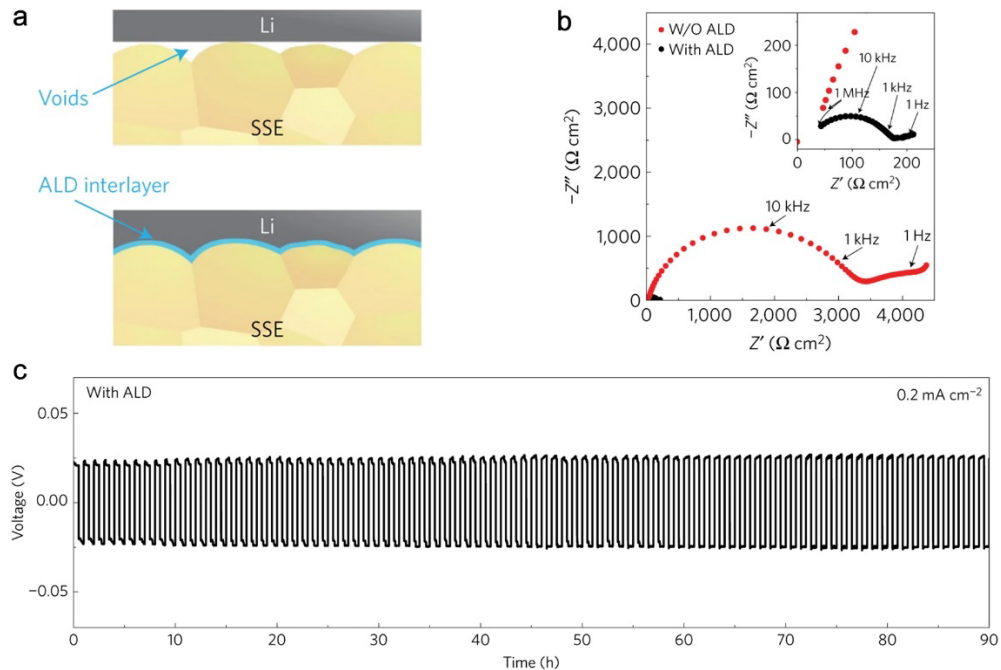


Figure 14-13. (a) Schematic of the wetting behavior of garnet surface with molten Li, (b) Comparison of EIS profiles of the symmetric Li non-blocking garnet cells. The inset shows the enlarged impedance curve of the ALD-treated garnet cell. (c) Galvanostatic cycling of Li/ALD-treated garnet/Li with a current density of 0.2 A cm^{-2} .⁷¹

After years of dedicated research, researchers have gained a deeper understanding of the fundamental issues and made progress in ASSBs. However, solid-state batteries still have unresolved scientific concerns: (1) the transport mechanism of Li-ions in the SSE is still not clearly defined and standardized, especially for the transport at the interface of the organic-inorganic composite SSE; (2) the multiphase interface of SSE/electrode is difficult to characterize due to the assembly method of the solid-state batteries, particularly to trace the interfacial reaction in real time; (3) the growth mechanism of lithium dendrites in SSEs is remaining controversial; (4) the charge-discharge behavior of solid-state batteries involves multiple temporal and spatial scales, which is a great challenge for both experimental characterization and theoretical studies. In the future, the further advancement of nanoscale and sub-nanoscale investigations such as ab initio molecular dynamic and in-operando electron microscopy may establish the ion transport constitutive relations and transport mechanisms in solid electrolytes, from the current schematic-only theory and will enhance the fundamentals of condensed-matter physics and guide the development of SSE materials.

4. Outlook

In this chapter, we provide an overview of nanotechnology applications in the field of LIBs, focusing particularly on their significant impact on the three fundamental components of batteries: the cathode, anode,

and electrolytes, respectively. The adoption of nanotechnology has notably enhanced the performance of LIBs, including but not limited to increasing energy density, improving charging and discharging efficiency, and enhancing cycle stability. Moreover, nanotechnology has played a crucial role in improving the safety of batteries, reducing the risks associated with overcharging and over-discharging.

As technology continues to advance, the application of nanotechnology is expected to broaden further, bringing more innovative possibilities to LIBs. We can anticipate that future lithium-ion batteries will be more compact, efficient, and safer. This is not only significant for the development of mobile electronic devices but also provides vital technological support for areas like new energy vehicles and large-scale energy storage systems.

In conclusion, the application of nanotechnology in LIBs is essential as a vibrant and promising strategy to continuously advance LIB performance, stability, and safety. It has not only propelled the innovation of battery technology but also had a profound impact on our lifestyle and energy consumption patterns. Looking ahead, as research deepens and technology matures, nanotechnology will continue to play an indispensable role in the field of LIBs, contributing to the realization of more sustainable and efficient energy solutions.

Reference:

1. Armand, M., and Tarascon, J. M., *Nature* (2008) **451** (7179), 652
2. Zhang, Y., *et al.*, *Nanoscale* (2023) **15** (9), 4195
3. Jiang, C., *et al.*, *Nano Today* (2006) **1** (4), 28
4. Manthiram, A., *Nature Communications* (2020) **11** (1), 1550
5. Kim, J. Y., *et al.*, *Energy Storage Materials* (2021) **41**, 289
6. Whittingham, M. S., *Nature Energy* (2021) **6** (2), 214
7. Seh, Z. W., *et al.*, *Nature Communications* (2014) **5** (1), 5017
8. Meini, S., *et al.*, *The Journal of Physical Chemistry Letters* (2014) **5** (5), 915
9. Trevey, J. E., *et al.*, *Journal of The Electrochemical Society* (2011) **158** (12), A1282
10. Walter, M., *et al.*, *Nanoscale* (2015) **7** (20), 9158
11. Zhang, Y., *et al.*, *Nano Energy* (2023) **115**, 108756
12. Mizushima, K., *et al.*, *Solid State Ionics* (1981), 171
13. Goodenough, J., *et al.*, *Japanese Journal of Applied Physics* (1980) **19**, 305
14. Goodenough, J. B., and Kim, Y., *Chemistry of Materials* (2010) **22** (3), 587
15. Aurbach, D., *et al.*, *Journal of Power Sources* (2007) **165** (2), 491
16. Tang, W., *et al.*, *Electrochemistry Communications* (2010) **12** (11), 1524
17. Xiao, X., *et al.*, *Nano Research* (2012) **5** (1), 27
18. Xiang, J., *et al.*, *RSC Advances* (2021) **11** (25), 14891
19. Kaur, G., and Gates, B. D., *Journal of The Electrochemical Society* (2022) **169** (4), 043504
20. Han, B., *et al.*, *ACS Applied Materials & Interfaces* (2017) **9** (17), 14769
21. Cho, J., *et al.*, *Electrochemical and Solid-State Letters* (1999) **2** (12), 607
22. Xie, M., *et al.*, *RSC Advances* (2016) **6** (68), 63250
23. Cho, J., *et al.*, *Chemistry of Materials* (2000) **12** (12), 3788
24. Wu, F., *et al.*, *ACS Applied Materials & Interfaces* (2015) **7** (6), 3773
25. Lee, Y., *et al.*, *Journal of Power Sources* (2016) **315**, 284
26. Min, K., *et al.*, *Scientific Reports* (2017) **7** (1), 7151
27. Hu, G.-R., *et al.*, *Electrochimica Acta* (2008) **53** (5), 2567
28. Sattar, T., *et al.*, *Scientific Reports* (2021) **11** (1), 18590
29. Gao, Y., *et al.*, *Journal of The Electrochemical Society* (2018) **165** (16), A3871
30. Lu, Y.-C., *et al.*, *Chemistry of Materials* (2009) **21** (19), 4408
31. Gao, X.-W., *et al.*, *Journal of Materials Chemistry A* (2015) **3** (1), 404
32. Bai, Y.-m., *et al.*, *Journal of Alloys and Compounds* (2010) **508** (1), 1
33. Gan, Q., *et al.*, *ACS Applied Materials & Interfaces* (2019) **11** (13), 12594
34. Zhang, Y., *et al.*, *Energy Storage Materials* (2022) **48**, 1
35. Xu, G.-L., *et al.*, *Nature Energy* (2019) **4** (6), 484
36. Zhang, Y., and Lee, S., *Applied Physics Letters* (2023) **123** (5), 050501
37. Zhang, W.-J., *Journal of Power Sources* (2011) **196** (6), 2962
38. Ravet, N., *et al.*, *Journal of Power Sources* (2001) **97-98**, 503
39. Takahashi, M., *et al.*, *Journal of Power Sources* (2001) **97-98**, 508
40. Yamada, A., *et al.*, *Journal of The Electrochemical Society* (2001) **148** (3), A224
41. Chen, S.-P., *et al.*, *Energy & Fuels* (2022) **36** (3), 1232
42. Mahmood, N., *et al.*, *Advanced Energy Materials* (2016) **6** (17), 1600374
43. Cheng, H., *et al.*, *Journal of Energy Chemistry* (2021) **57**, 451
44. Goriparti, S., *et al.*, *Journal of Power Sources* (2014) **257**, 421
45. Zhang, H., *et al.*, *Energy Storage Materials* (2021) **36**, 147
46. Yamada, Y., *et al.*, *Nature Energy* (2019) **4** (4), 269
47. Ni, K., *et al.*, *Advanced Materials* (2019) **31** (23), 1808091
48. Li, S., *et al.*, *Advanced Functional Materials* (2022) **32** (23), 2200796
49. Prakash, A. S., *et al.*, *Chemistry of Materials* (2010) **22** (9), 2857

50. Zhu, G.-N., *et al.*, *Energy & Environmental Science* (2011) **4** (10), 4016
51. Sandhya, C. P., *et al.*, *Ionics* (2014) **20** (5), 601
52. Li, P., *et al.*, *Energy Storage Materials* (2018) **15**, 422
53. Zuo, X., *et al.*, *Nano Energy* (2017) **31**, 113
54. Li, J.-Y., *et al.*, *Materials Chemistry Frontiers* (2017) **1** (9), 1691
55. Chan, C. K., *et al.*, *Nature Nanotechnology* (2008) **3** (1), 31
56. Liu, N., *et al.*, *Nature Nanotechnology* (2014) **9** (3), 187
57. Franco Gonzalez, A., *et al.*, *The Journal of Physical Chemistry C* (2017) **121** (50), 27775
58. Cheng, X.-B., *et al.*, *Chemical Reviews* (2017) **117** (15), 10403
59. Li, Q., *et al.*, *Green Energy & Environment* (2016) **1** (1), 18
60. Verma, P., *et al.*, *Electrochimica Acta* (2010) **55** (22), 6332
61. Zheng, F., *et al.*, *Journal of Power Sources* (2018) **389**, 198
62. Bhattacharyya, A. J., and Maier, J., *Advanced Materials* (2004) **16** (9-10), 811
63. Scrosati, B., and Vincent, C. A., *MRS Bulletin* (2000) **25** (3), 28
64. Li, S., *et al.*, *Advanced Science* (2020) **7** (5), 1903088
65. Zhao, Q., *et al.*, *Nature Reviews Materials* (2020) **5** (3), 229
66. Manthiram, A., *et al.*, *Nature Reviews Materials* (2017) **2** (4), 16103
67. Zhao, C.-Z., *et al.*, *Proceedings of the National Academy of Sciences* (2017) **114** (42), 11069
68. Salomon, M., *Journal of Solution Chemistry* (1993) **22** (8), 715
69. Ue, M., *Journal of The Electrochemical Society* (1994) **141** (12), 3336
70. Chen, L., *et al.*, *Nano Energy* (2018) **46**, 176
71. Han, X., *et al.*, *Nature Materials* (2017) **16** (5), 572